Experimental study of the influence of nitrogen and oxygen on the solubility of solid carbon dioxide in liquid and vapor methane at low temperature

Paolo Stringari, Mauro Riva

Experimental study of the influence of nitrogen and oxygen on the solubility of solid carbon dioxide in liquid and vapor methane at low temperature

*Mauro Riva†‡, Paolo Stringari†**

†MINES ParisTech, PSL Research University, CTP - Centre of Thermodynamics of Processes, 35 rue St Honoré, 77300 Fontainebleau, France

‡Cryo Pur, 3 rue de la Croix Martre, 91120 Palaiseau, France

KEYWORDS. Solid-liquid-vapor equilibrium, Solubility, Biogas, Natural Gas, LNG, BioLNG, Cryogenics, Measurements.

ABSTRACT

Undesired solid CO_2 formation is a main issue for the liquefied natural gas (LNG) industry and, more recently, for the bioLNG production. The abundance of CO_2 solubility data in liquid methane may not be sufficient to fully understand the problem when important amount of air gases (O_2 and N_2) are present in the natural gas or biomethane. Scarcity and incompleteness of available solubility data involving nitrogen and oxygen motivated the production of original solid-liquid-vapor equilibrium (SLVE) data for the N_2-CH_4-CO_2 and N_2-O_2-CH_4-CO_2 systems. The solubility limit of CO_2 in both liquid and vapor phases is measured in this work in order to allow the definition of solid formation conditions. A static analytic methodology is used for obtaining (p,T,x,y) data at SLVE in the temperature range from 125 to 146 K. Experimental results obtained in this work show that the addition of nitrogen and oxygen in methane decreases the solubility of CO_2 in the liquid phase, which is not in agreement with the qualitative behavior shown by literature data. A thermodynamic model for the calculation of solid-liquid-vapor equilibrium of the N_2-O_2-CH_4-CO_2 system is also presented in this work and compared with experimental data, providing good agreement.

1. INTRODUCTION

The study of the influence of nitrogen and air content on the production of liquefied methane is of great importance for the development of new technologies in the field of LNG or alternative liquid fuels, such as the bioLNG (or liquefied biomethane). Nitrogen is a classical natural gas impurity, usually treated only after liquefaction in the Nitrogen Rejection Unit. The interest on biomethane as an advanced liquid bio-fuel has grown over the past decade, driven by decarbonisation objectives in recent energy policy. Raw biogas produced by anaerobic digestion of organic substrate (agricultural wastes, water treatment and landfill wastes) is mainly composed of methane and carbon dioxide. In some cases air is present in the raw biogas: in biogas produced in landfills (landfill gas), which is originated by spontaneous degradation of organic substances present in wastes, air is seeped into the biogas pipes during the collection process and can represent up to 20% of the volume fraction. Also in the biogas digesters some air can be injected (up to 8%) in order to reduce the hydrogen sulfide production through bacterial oxidation, the so-called biological desulfurization.

Liquefied biomethane is produced at temperature similar to the Liquefied Natural Gas operating conditions, but at lower pressure, usually lower than 3 MPa. During the liquefaction process, CO_2 solidification may occur from both the vapor and liquid phase. The prediction of solid formation conditions from vapor and liquid phases is thus of essential importance for the design and simulation of the liquefaction process, in order to avoid uncontrolled solid formation. Solid CO_2 solubility in liquid and vapor phases can be calculated by means of appropriate thermodynamic models able to compute the phase equilibrium involving a solid phase. Nevertheless, phase equilibrium measurements are needed for the regression of model parameters and for the validation of the model.

A large number of experimental studies provide the CO_2 solubility in liquid and vapor methane in the range of interest, going from the boiling temperature of LNG/bio LNG at atmospheric pressure (around 110 K) to the boiling temperature at liquefaction pressure (around 180 K), and some studies also provide the solubility of carbon dioxide in nitrogen and oxygen, as shown in Table 1. CO_2 solubility in liquid phase is the CO_2 content in liquid phase at the solid-liquid equilibrium (SLE). SLE data usually provide temperature and composition of the liquid phase, but rarely the pressure. CO_2 solubility in vapor phase is the CO_2 content in vapor phase at the solid-vapor equilibrium (SVE). When solid phase is in equilibrium with coexisting vapor and liquid phase the phase equilibrium is called solid-liquid-vapor equilibrium (SLVE). The phase diagram of ternary N_2-CH_4-CO_2 system involving a solid phase has been only partially determined through experimental data. An analysis of the experimental procedure and comparison with model results obtained at same temperature, pressure and global composition, show some incompleteness in available data: declared SLE data[1,2], are actually SLVE data providing only the CO_2 composition in the liquid phase. Furthermore no data for the quaternary mixture N_2-O_2-CH_4-CO_2 are available, to the authors' knowledge.

The qualitative phase diagram in Figure 1 is representative of the behavior of the N_2-CH_4-CO_2 mixture in the range of temperature and pressure of interest and can help understanding the problem of undesired solid CO_2 formation during methane liquefaction. Considering the stable phases for the pure components at the temperature and pressure of the measurements carried out in this work, CO_2 is in solid phase, CH_4 is in liquid phase and N_2 is in vapor phase. A mixture of methane and carbon dioxide thus presents a solid-liquid equilibrium (SLE) where solid CO_2 is solubilized in the liquid phase. In the ternary diagram, there is thus a SLE region when the system is rich in methane and carbon dioxide, but poor in nitrogen. On the contrary, when the

system is rich in nitrogen and carbon dioxide, but poor in methane, the system is in the SVE region. If the amount of CO_2 is small, no solid is formed and the mixture rich in N_2 and CH_4 is thus in vapor or liquid phase, or at vapor-liquid equilibrium conditions. The SLE, SVE and VLE regions delimit the SLVE triangular region, where the composition of each phase is defined by the vertices of the triangle: in the studied case, solid phase is pure CO_2, vapor phase is the vertex with higher N_2 concentration and the liquid phase is the vertex with higher CH_4 concentration. The composition of the phases at SLVE does not depend on the global composition of the system for a ternary system at given T and p. From the study of the ternary phase diagram, one can observe that for assuring that a multicomponent system containing methane and carbon dioxide does not present the risk of solid formation at given temperature, pressure and global composition, it can be not sufficient to check the solubility of the carbon dioxide in the liquid phase. In Figure 1, point A represents a mixture with CO_2 content lower than the CO_2 solubility limit in liquid phase and poor in nitrogen: no solid phase is formed from this mixture at given T and p. Point B represents a mixture with same CO_2 content but richer in N_2. Point B falls in the SLVE region and thus a solid phase is present, in equilibrium with a liquid and a vapor phase. It is then evident that, in order to evaluate the potential formation of solid CO_2 in the natural gas or biomethane liquefaction, a precise knowledge of the position of the phase boundaries is mandatory. This consideration is valid for both the N_2-CH_4-CO_2 and the N_2-O_2-CH_4-CO_2 systems. For improving the comprehension of these complex multicomponent systems at conditions where a solid phase can appear, original SLVE measurements in the low temperature region are thus produced in this work.

2. EXPERIMENTAL SETUP AND PROCEDURE

2.1 Experimental setup

The apparatus used in this work for obtaining low temperature SLVE measurements for the N_2-CH_4-CO_2 mixture and N_2-O_2-CH_4-CO_2 mixture is a slightly modified version of the original apparatus used for low temperature vapor-liquid equilibrium (VLE) measurements [20] and solubility data [17, 21]. Recently the apparatus has been used for determining solid formation conditions [22].

A scheme of the apparatus is represented in Figure 2. The equilibrium cell (EC) is placed into a 55 liters Dewar, partially filled with liquid nitrogen (LN2). In this way, the cell is surrounded by a nitrogen vapor atmosphere. The equilibrium cell is surrounded by a brass shell closed with a brass cap. The brass shell is wrapped by an electric resistance regulated by a Fuji electric PXR PID temperature regulator. The cold source (liquid nitrogen) coupled with the electric resistance allows temperature regulation in the cell. The liquid nitrogen is supplied from a 176 liters ranger intended for this purpose. The temperature is measured at the top and at the bottom of the cell by means of two PT100Ω (at 0°C) temperature probes, in order to estimate the temperature gradient between the top and the bottom of the cell and induced by the position of the cold source. The average temperature between the two probes is calibrated on the saturated curves of pure methane and pure oxygen. The pressure in the EC is measured by two PTX611 Druck pressure transducers, one for nominal maximum pressure up to 16 MPa and the other up to 0.16 MPa (this last can be isolated when working pressure is higher than 0.16 MPa). Temperature and pressure calibration procedures are discussed in the Supporting Information. The cell is equipped with two pneumatic ROLSI® samplers with stainless steel capillaries. The temperature of the part of

the liquid capillary between the cell and the ROLSI® samplers is controlled by a heating cartridge connected to a PID regulator in order to avoid undesired solidification and condensation during the sampling operations. The ROLSI® samplers are connected to the Gas Chromatograph (GC) through a thermostated transfer line. The GC device is a Perichrom PR 2100 type equipped with a Thermal Conductivity Detector (TCD) and a Flame Ionisation Detector (FID) for analyzing the composition. A Porapak Q column (80/100 mesh, 1/8" external diameter, 2 mm internal diameter, length depending on the system to study, made in Silcosteel), is used for separating the mixture components in the gas chromatograph. Operational conditions of the GC are resumed in Table 2. The CO_2 content in fluid phases at low temperature SLVE is expected to be in the range from 20 to 10000 ppm. The Thermal Conductivity Detector (TCD) is not sensitive enough for revealing the lowest CO_2 quantities in such a range. As a consequence, the detection of small amounts of CO_2 is performed by a Flame Ionisation Detector (FID). Since the FID cannot directly detect CO_2, a methanizer is installed for reducing CO_2 into methane, which can be detected by the FID. The methanizer is a U-tube containing nickel catalyst and kept at 300°C for allowing the complete conversion of CO_2 into CH_4. The four gases used in this work are provided by Air Liquide with declared purity of 99.995%, except for oxygen with declared purity of 99.999%.

2.2 Experimental procedure

A static analytic approach is used for determining the SLVE data at low temperature for the N_2-CH_4-CO_2 mixture and N_2-O_2-CH_4-CO_2 mixture. In order to determine temperature, pressure, liquid and vapor phase compositions at SLVE conditions, the adopted procedure is composed of three main steps: the loading of the cell, the cooling program for reaching the desired

temperature where solid is expected to form, the composition analysis of liquid and vapor phases.

Once vacuum is obtained into the equilibrium cell thanks to a vacuum pump, the mixture with desired composition is loaded into the cell at ambient temperature. Each pure component is loaded into the cell separately from a gas cylinder. The cell is then isolated and the magnetic stirrer activated for assuring suitable mixing in the cell. Once temperature and composition in the equilibrium cell become stable (i.e. their variation in time is lower than the experimental uncertainty in measuring these quantities), the global composition of the loaded mixture is determined by GC analysis.

After the loading of the cell, the Dewar is filled with liquid nitrogen at the half of its volume, avoiding the contact between the bottom of the cell and the liquid nitrogen. The temperature and the pressure inside the cell are continuously recorded and the system is cooled down by setting the temperature regulator. A first rapid cooling is performed down to a temperature set 5 K higher than the expected solid formation temperature. When the system stably reaches this temperature, a second slow cooling is executed setting the temperature regulator to 146 K. The cooling rate is set to 0.5 K/h, and once the temperature is reached, the system is kept at stable temperature for around 48h, checking the stability of pressure. At the end of this period, vapor and liquid phases are sampled for the composition analysis. A series of different samples are analyzed in order to assess the repeatability of the composition measurement. At least two series of samples are taken and analyzed at significant time distance for assuring the stability of the composition. Once the procedure for liquid and vapor phase composition measurement is successfully completed, the Dewar is refilled with liquid nitrogen and temperature is slowly decreased setting the temperature regulator to 132 K with same cooling rate (0.5 K/h). The

system is thus kept at stable temperature for around 48h, and composition analysis of vapor and liquid phase is performed following the procedure previously described. After that, the Dewar is refilled and temperature is decreased setting the temperature regulator to 125 K with same cooling rate (0.5 K/h) for another composition analysis. The temperature of the cell is then let increasing up to ambient temperature for evacuating the cell and loading a new mixture. The procedure is repeated for four different mixtures, with compositions reported in Table 3.

3. RESULTS AND DISCUSSION

3.1 Experimental Results

For each of the four different series of measurements, namely four different global composition mixtures, the measured composition (mole fraction) of liquid and vapor phases and estimated uncertainties at each temperature and pressure are reported in Table 4. Expanded uncertainty (coverage factor equal to 2) on temperature is estimated to be 0.2 K and expanded uncertainty (coverage factor equal to 2) on pressure 0.003 MPa. Details on calculations of uncertainties are presented in the Supporting Information. The formation of a solid phase at experimental temperature and pressure can be inferred from the material balance on CO_2:

$$S = z_{CO2} - y_{CO2}V - x_{CO2}L \quad (1)$$

with:

$$V + L + S = 1 \quad (2)$$

where z_{CO2} is the global CO_2 mole fraction of the loaded mixture (known), y_{CO2} and x_{CO2} are the measured CO_2 mole fractions in the vapor and liquid phases and V, L and S the mole fractions of

vapor, liquid and solid respectively. The solid phase is assumed to be pure CO_2. Being z_{CO2} significantly greater than x_{CO2} and y_{CO2} in the measurements performed in this work (see Table 3 and Table 4), one obtains a value of S greater than 0 when replacing the experimental values in eq. (1) and eq. (2), proving that a solid phase is present. Values of S for each measurement are reported in Section 3 of the Supporting Information.

Figure 3 presents a qualitative comparison among the experimental results obtained in this work for CO_2-CH_4-N_2 and CO_2-CH_4-N_2-O_2 and the literature data of CO_2 solubility for the binary mixture CO_2-CH_4 and CO_2-CH_4-N_2 as function of temperature. The comparison is only qualitative because the solubility of solid CO_2 in the liquid phase depends also on the pressure of the measurements and on the mole fraction of nitrogen in the liquid phase. Nevertheless, it is possible to observe that the addition of nitrogen and oxygen in methane decreases the solubility of CO_2 in the liquid phase in the temperature range investigated. The effect can be explained studying the CO_2 solubility in liquid oxygen and nitrogen, which is lower than in liquid methane, according to literature data presented in Tab. 1. In the investigated temperature range, one can conclude that methane mole fraction in liquid phase has a major effect on CO_2 solubility in liquid phase. When some nitrogen and oxygen are added to methane, methane mole fraction in liquid phase decreases and thus the CO_2 solubility decreases too. The quantitative comparison with the other literature data for the mixture CO_2-CH_4-N_2 is not possible because of the differences in pressure and nitrogen mole fraction of the measurements.

3.2 Model for SLVE calculation

Obtained experimental values can be compared with data from literature, when available, and with model results. The approach chosen for modeling the SLVE is the isofugacity of the solid former component in liquid (f_{CO2}^{L}), vapor (f_{CO2}^{V}) and solid phase (f_{CO2}^{S}), which can be assumed as pure CO_2.

$$f_{CO2}^{L}(T,p,\boldsymbol{x}) = f_{CO2}^{V}(T,p,\boldsymbol{y}) = f_{CO2}^{S}(T,p) \quad (3)$$

Where T is the temperature, p the pressure, $\boldsymbol{x}$ and $\boldsymbol{y}$ the vectors of compositions of the liquid and vapor phase respectively.

The fugacity of the solid phase can be calculated from the model developed for the solid CO_2 by Jäger and Span[23]. The advantage of this model is that the fugacity of the solid CO_2 can be directly calculated from the EoS, without any derivation from a hypothetical subcooled liquid fugacity.

$$f_{CO2}^{S}(T,p) = p^{0}\exp\left(\frac{g_{CO2}^{S}(T,p) - g_{CO2}^{0}(T,p)}{RT}\right) \quad (4)$$

The suffix 0 is for the reference state, taken in this work as ideal gas at $p^0 = 0.101325\ MPa$ and $T^0 = 150\ K$. g_{CO2}^{0} is thus the ideal gas Gibbs free energy, which can be obtained from the reference quality Eos for pure CO_2, reported in Kunz et al. (2007) [24].

It has been chosen to compute the fugacity of the fluid phases from the GERG 2008 Equation of State (GERG 2008 EoS), providing high accuracy in representing phase equilibria and thermodynamic properties of natural gas type mixtures in liquid and vapor phases [24, 25]. In this work, the models for both the solid and the fluid fugacities have been used with the original parameters available from the literature [23-25].

The range of validity of an empirical equation of state is, typically, determined by the available data used for regressing the equation parameters. In particular for the CH_4-CO_2 system, data for the fluid phases are available down to 153 K[26] and for the N_2-CO_2 system down to 209 K[27]. Nevertheless the GERG 2008 multi-parameter EoS is developed in order to behave reasonably far beyond the range of temperature and pressure of existing data [24]. Still, data for the O_2-CH_4 system are not available and then EoS parameters are not regressed for this system. As a consequence, the model is predictive when dealing with the N_2-O_2-CH_4-CO_2 system. Experimental CO_2 solubility in liquid and vapor phase obtained in this work is tabulated in Table 5, together with solubility calculated from the model at experimental temperature, pressure and global composition. The measured CO_2 solubility in liquid phase is lower than solubility obtained by the model at experimental temperature, pressure and global composition: CO_2 solubility in liquid phase is overestimated by the model, as it is possible to see in Figure 4. From both model and experimental results it is possible to observe that CO_2 solubility in liquid phase slightly decreases with decreasing pressure. From Figure 5 it is possible to observe that, according to experimental values, CO_2 solubility in vapor phase increases when some nitrogen is replaced by oxygen, but the phenomenon is not predicted by the model. Unfortunately, no SVE data are available for the O_2-CO_2 system for comparing the solubility of methane in vapor oxygen or nitrogen.

The thermodynamic model allows pointing out the dependence of CO_2 solubility on the density of the solvent. In Figs. 6, 7a, and 7b, the solubility of each series of measurements has been plotted as a function of the density calculated by the thermodynamic model at the experimental temperature, pressure, and CO_2-free mole fraction of the liquid phase (Fig. 6) and of the vapor phase (Figs. 7a and 7b). Fig. 6 allows inferring that, for each series of measurements (i.e. for

each global composition of the mixture, see Tab. 3), the solubility of CO_2 in the liquid phase decreases when density increases. The trend of solubility of CO_2 with respect to the density of the solvent is very similar for the two series 1 and 2 obtained for the N_2-CH_4-CO_2 mixture (full and empty squares in Fig. 6). Also the two series 3 and 4 obtained for the N_2-O_2-CH_4-CO_2 mixture (full and empty triangles in Fig. 6) present a similar behavior. The solubility of CO_2 with respect to the calculated density of the solvent (CO_2-free) in the vapor phase is plotted in Fig. 7a for mixture N_2-CH_4-CO_2, and in Fig. 7b for mixture N_2-O_2-CH_4-CO_2. Also in this case it is possible to observe a very similar behavior of the solubility of CO_2 with respect to the density of the solvent for the series 1 and 2, Fig. 7a, and 3 and 4, Fig. 7b.

Expanded uncertainties (coverage factor equal to 2) associated to the mole fraction values are reported in Tab. 4. For methane, the uncertainty is always lower than 2% of the mole fraction value in the liquid phase and 4% in the vapor phase. For oxygen it is lower than 30% of the mole fraction value in the liquid phase and 8% in the vapor phase. For carbon dioxide, it is lower than 20% of the mole fraction (ppm) value in the liquid phase and 50% in the vapor phase.

CONCLUSIONS

In this work, low temperature phase behavior of the methane-carbon dioxide system with addition of air (nitrogen and oxygen) is studied thanks to original SLVE experimental measurements and data from literature. The study is important for understanding the solid formation conditions and maximum CO_2 allowable content in the LNG and bioLNG production processes, especially when significant amount of air gases are present. For this purpose, the study of the SLE may not be sufficient because the presence of light component (N_2 and O_2) induce the formation of a vapor phase at conditions where no vapor phase exists for the binary

CH_4-CO_2 system. Furthermore, from experimental results obtained in this work, it is possible to conclude that the addition of nitrogen and oxygen in methane decreases the solubility of CO_2 in the liquid phase, for temperatures between 125 and 145 K. More experimental studies are suggested in order to provide a full description of the system behavior as function of temperature, pressure, and nitrogen and/or oxygen mole fraction.

Experimental measurements are necessary for testing and calibrating thermodynamic models able to provide a complete representation of the phase behavior of complex systems. The model presented in this work, coupling a high accuracy EoS for the fluid phase (GERG 2008) and an EoS specifically developed for solid CO_2, agrees with experimental values, even if it overestimates the CO_2 solubility in liquid phase.

TABLES.

Table 1. Selected experimental data sources for the CO_2 solubility in liquid and vapor phase in the temperature range 110-180 K.

Author	Mixture	Kind of data	N	Info
Shen et al.(2012) [1]	CH_4-CO_2	SLVE	9	Tpx
	N_2-CH_4-CO_2	SLVE	27	Tpx_{CO2}
Gao et al. (2012) [2]	CH_4-CO_2	SLVE	9	Tx
	N_2-CH_4-CO_2	SLVE	31	Tpx_{CO2}
Davis et al. (1962) [3]	CH_4-CO_2	SLVE	42	Tp,Tx,Ty
Boyle (1987)[4]	CH_4-CO_2	SLE	5	Tx
Cheung and Zander (1968) [5]	CH_4-CO_2	SLE	9	Tx
Streich (1970) [6]	CH_4-CO_2	SLE	12	Tx
Preston et al. (1971)[7]	CH_4-CO_2	SLE	2	Tx
Voss (1975)[8]	CH_4-CO_2	SLE	22	Tx
Pikaar (1959) [9]	CH_4-CO_2	SVE	103	Tpy
		SLE	21	Tpx
Yakimenko et al. (1975) [14]	N_2-CO_2	SLE	9	Tx
Agrawal and Leverman (1974) [10]	CH_4-CO_2	SVE	41	Tpy
	N_2-CH_4-CO_2	SVE	19	Tpy
Le and Trebble (2007) [11]	CH_4-CO_2	SVE	55	Tpy
	N_2-CH_4-CO_2	SVE	24	Tpy
Xiong et al. (2015) [12]	CH_4-CO_2	SVE	64	Tpy
	N_2-CH_4-CO_2	SVE	77	Tpy
Fedorova (1940) [13]	N_2-CO_2	SLE	4	Tx
	O_2-CO_2	SLE	5	Tx
Yakimenko et al. (1975) [14]	N_2-CO_2	SLE	9	Tx

Amamchyan et al. (1973) [15]	O_2-CO_2	SLE	7	Tx
Rest et al. (1990) [16]	N_2-CO_2	SLE	5	Tx
	O_2-CO_2	SLE	3	Tx
De Stefani et al. (2002)[17]	O_2-CO_2	SLE	13	Tx
Sonntag and Van Wilen (1961)[18]	N_2-CO_2	SVE	64	Tpy
Smith et al. (1964) [19]	N_2-CO_2	SVE	72	Tpy

Table 2. Gas Chromatography operating conditions used in this work

Mixture	N_2-CH_4-CO_2	N_2- O_2-CH_4-CO_2
Column	4m Porapak Q	2x4m Porapak Q
Oven Temperature	343 K	248 K for 6.5 min 343 K for 14 min
N_2 retention time (min)	0.9	5.3
O_2 retention time (min)	-	6.3
CH_4 retention time (min)	1.25	10.2
CO_2 retention time (min)	2.5	16
Carrier gas	He	He
Carrier flow (ml/min)	21	21
TCD temperature	393 K	393 K
FID temperature	573 K	573 K
H_2 flow in the methanizer	30 ml/min	30 ml/min

Table 3. Global composition of loaded mixture for each series of measurements. N is the series of measurements.

N	N_2 mol/mol	O_2 mol/mol	CH_4 mol/mol	CO_2 mol/mol
1	0.4	-	0.58	0.02
2	0.19	-	0.79	0.02
3	0.31	0.09	0.58	0.02
4	0.15	0.04	0.79	0.02

Table 4. SLVE experimental liquid (x) and vapor (y) compositions measured in this work for the mixture of N_2 (1)-O_2 (2)-CH_4 (3)-CO_2 (4) and corresponding expanded uncertainties U (coverage factor equal to 2). N is the series of measurements, corresponding to the global composition reported Table 3

N	T (K)	P (MPa)	x_2	$U(x_2)$	x_3	$U(x_3)$	x_4 (ppm)	$U(x_4)$ (ppm)	y_2	$U(y_2)$	y_3	$U(y_3)$	y_4 (ppm)	$U(y_4)$ (ppm)
1.1	145.9	2.04	-	-	0.763	0.008	6909	900	-	-	0.387	0.012	470	26
1.2	132.1	1.36	-	-	0.734	0.010	1632	331	-	-	0.264	0.009	48	15
1.3	124.9	0.77	-	-	0.705	0.010	749	59	-	-	0.205	0.008	16	8
2.1	145.8	1.12	-	-	0.885	0.005	5722	736	-	-	0.558	0.011	572	22
2.2	132.1	0.77	-	-	0.902	0.004	1185	148	-	-	0.470	0.012	51	12
2.3	124.5	0.52	-	-	0.919	0.004	532	39	-	-	0.444	0.012	15	5
3.1	146.1	2.11	0.070	0.004	0.743	0.005	6948	78	0.119	0.006	0.385	0.006	1542	28
3.2	132.4	1.35	0.083	0.006	0.704	0.012	1709	48	0.129	0.004	0.268	0.004	209	4
3.3	125	0.96	0.084	0.006	0.708	0.007	367	27	0.133	0.005	0.227	0.004	46	9
4.1	146.5	1.39	0.027	0.006	0.891	0.007	6547	217	0.072	0.006	0.599	0.013	1392	41
4.2	132.5	0.84	0.032	0.010	0.884	0.013	1544	90	0.088	0.004	0.468	0.006	185	5
4.3	125.1	0.58	0.033	0.005	0.880	0.006	356	27	0.091	0.003	0.414	0.003	35	2

Table 5. Measured and calculated CO_2 solubility in liquid (x_{CO2}) and vapor phase (y_{CO2}) and deviation between measured and calculated values.

N	T	P	$x_{CO2,EXP}$	$x_{CO2,CALC}$	Δx_{CO2}	$y_{CO2,EXP}$	$y_{CO2,CALC}$	Δy_{CO2}
	(K)	(MPa)	(ppm)	(ppm)	(ppm)	(ppm)	(ppm)	(ppm)
1.1	145.9	2.04	6909	7846	937	470	633	163
1.2	132.1	1.36	1632	2853	1221	48	92	44
1.3	124.9	0.77	749	1573	824	16	28	12
2.1	145.8	1.12	5722	7674	1952	572	689	117
2.2	132.1	0.77	1185	2669	1484	51	120	69
2.3	124.5	0.52	532	1349	817	15	40	25
3.1	146.1	2.11	6948	7831	883	1542	631	-911
3.2	132.4	1.35	1709	2901	1192	209	96	-113
3.3	125	0.96	367	1551	1184	46	30	-16
4.1	146.5	1.39	6547	7986	1439	1392	750	-642
4.2	132.5	0.84	1544	2787	1243	185	121	-64
4.3	125.1	0.58	356	1451	1095	35	41	6

ASSOCIATED CONTENT

Supporting Information.

Additional details on the calibration procedures for temperature, pressure and CG analysis; uncertainties calculation for temperature, pressure and composition

AUTHOR INFORMATION

Corresponding Author

*E-mail: paolo.stringari@mines-paristech.fr

ABBREVIATIONS

LNG, liquefied natural gas; bioLNG, liquefied biomethane; SLE, solid-liquid equilibrium; SVE, solid-vapor equilibrium; VLE, vapor-liquid equilibrium; SLVE, solid-liquid-vapor equilibrium; EoS, equation of state; GC, Gas Chromatography; LN2, liquid nitrogen.

REFERENCES

(1) Shen, T.; Gao, T.; Lin, W.; Gu, A. Determination of CO_2 Solubility in Saturated Liquid CH_4 + N_2 and CH_4 + C_2H_6 Mixtures above Atmospheric Pressure. *J. Chem. Eng. Data* **2012**, *57*, 2296–2303.

(2) Gao, T.; Shen, T.; Lin, W.; Gu, A.; Ju, Y. Experimental Determination of CO_2 Solubility in Liquid CH_4/N_2 Mixtures at Cryogenic Temperatures. *Ind. Eng. Chem. Res.* **2012**, *51*, 9403–9408.

(3) Davis, J. A.; Rodewald, N.; Kurata, F. Solid-Liquid-Vapor Phase Behavior of the Methane-Carbon Dioxide System. *AIChE J.* **1962**, *8*, 537–539.

(4) Boyle, G. J. Shell Res. LTD Thornton Res. Centre P. O. Box. 1 Chester. Rep. Knapp H.; Teller M.; Langhorst R. *Solid-Liq. Equilib. Data Collect. Vol VIII Part 1 Chem. Data Ser.* Dechema: Frankfurt am Main, 1987.

(5) Cheung, H.; Zander, E. H. Solubility of Carbon Dioxide and Hydrogen Sulfide in Liquid Hydrocarbons at Cryogenic Temperatures. *Chem. Eng. Prog. Symp. Ser.* **1968**, *64*, 34–43.

(6) Streich, M. N_2 Removal from Natural Gas. *Hydrocarb. Process.* **1970**, *49*, 86–88.

(7) Preston, G. T.; Funk, E. W.; Prausnitz, J. M. Solubilities of Hydrocarbons and Carbon Dioxide in Liquid Methane and in Liquid Argon. *J. Phys. Chem.* **1971**, *75*, 2345–2352.

(8) Voss, G. PhD Thesis, Technical University of Berlin: Berlin, Germany, 1975. Rep. Knapp H.; Teller M.; Langhorst R. *Solid-Liq. Equilib. Data Collect. Vol VIII Part 1 Chem. Data Ser.* Dechema: Frankfurt am Main, 1987.

(9) Pikaar, M. J. *Study of Phase Equilibria in Hydrocarbon-CO_2 Systems*. PhD Thesis, Imperial College of Science and Technology: London, 1959.

(10) Agrawal, G. M.; Laverman, R. J. Phase Behavior of the Methane-Carbon Dioxide System in the Solid-Vapor Region. CO2-CH4 and N2-CH4-CO2 Mixtures at Compositions and Pressures of Industrial Importance. *Adv. Cryog. Eng.* **1974**, *19*, 327–338.

(11) Le, T. T.; Trebble, M. A. Measurement of Carbon Dioxide Freezing in Mixtures of Methane, Ethane, and Nitrogen in the Solid-Vapor Equilibrium Region. *J. Chem. Eng. Data* **2007**, *52*, 683–686.

(12) Xiong, X.; Lin, W.; Jia, R.; Song, Y.; Gu, A. Measurement and Calculation of CO_2 Frost Points in CH_4 + CO_2/CH_4 + CO_2 + N_2/CH_4 + CO_2 + C_2H_6 Mixtures at Low Temperatures. *J. Chem. Eng. Data* **2015**, *60*, 3077–3086.

(13) Fedorova, M. F. The Solubility of C_2H_2 and CO_2 in Liquid Nitrogen and Oxygen. *Zhurnal Fiz. Khimii* **1940**, *14*, 422–426.

(14) Yakimenko, N. P.; Gluch, G. M.; Iomtev, M. B.; Abramova, R. I. Solubility of Solid Carbon-Dioxide in Liquid-Nitrogen. *Zhurnal Fiz. Khimii* **1975**, *49*, 209–210.

(15) Amamchyan, R. G.; Bertsev, V. V.; Bulanin, M. O. Analysis of Cryogenic Solutions According to IR Absorption Spectra. *Zavod Lab* **1973**, *39*, 432–434.
(16) Rest, A. J.; Scurlock, R. G.; Wu, M. F. The Solubilities of Nitrous Oxide, Carbon Dioxide, Aliphatic Ethers and Alcohols, and Water in Cryogenic Liquids. *Chem. Eng. J.* **1990**, *43*, 25–31.
(17) De Stefani, V.; Baba-Ahmed, A.; Valtz, A.; Meneses, D.; Richon, D. Solubility Measurements for Carbon Dioxide and Nitrous Oxide in Liquid Oxygen at Temperatures down to 90 K. *Fluid Phase Equilibr.* **2002**, *200*, 19–30.
(18) Sonntag, R. E.; Van Wilen, G. J. The Solid-Vapor Equilibrium of Carbon Dioxide-Nitrogen. *Adv. Cryog. Eng.* **1961**, *7*, 99–105.
(19) Smith, G. E.; Sonntag, R. E.; Wylen, G. J. V. Solid-Vapor Equilibrium of the Carbon Dioxide-Nitrogen System at Pressures to 200 Atmospheres. *Adv. Cryog. Eng.* **1964**, *9*, 197–206.
(20) Baba-Ahmed, A.; Guilbot, P.; Richon, D. New Equipment Using a Static Analytic Method for the Study of Vapour–liquid Equilibria at Temperatures down to 77 K. *Fluid Phase Equilibria* **1999**, *166*, 225–236.
(21) Stringari, P.; Theveneau, P.; Coquelet, C.; Lauermann, G. Solubility Measurements of Solid N-Hexane in Liquid Methane at Cryogenic Temperature. 91st Annu. Conv. GPA New Orleans 2012.
(22) Lange, S. Purification of Natural Gas by Means of a New Low Temperature Distillation Process. PhD Thesis, Politecnico di Milano: Milano, 2015.
(23) Jäger, A.; Span, R. Equation of State for Solid Carbon Dioxide Based on the Gibbs Free Energy. *J. Chem. Eng. Data* **2012**, *57*, 590–597.
(24) Kunz, O.; Klimeck, R.; Wagner, W.; Jaeschke, M. The GERG-2004 Wide-Range Equation of State for Natural Gases and Other Mixtures, GERG TM15; VDI Verlag GmbH: Düsseldorf, 2007.
(25) Kunz, O.; Wagner, W. The GERG-2008 Wide-Range Equation of State for Natural Gases and Other Mixtures: An Expansion of GERG-2004. *J. Chem. Eng. Data* **2012**, *57*, 3032–3091.
(26) Mraw, S. C.; Hwang, S.-C.; Kobayashi, R. Vapor-Liquid Equilibrium of the Methane-Carbon Dioxide System at Low Temperatures. *J. Chem. Eng. Data* **1978**, *23*, 135–139.
(27) Duarte-Garza, H. A.; Holste, J. C.; Hall, K. R.; Marsh, K. N.; Gammon, B. E. Isochoric PVT and Phase Equilibrium Measurements for Carbon Dioxide + Nitrogen. *J. Chem. Eng. Data* **1995**, *40*, 704–711.

FIGURES

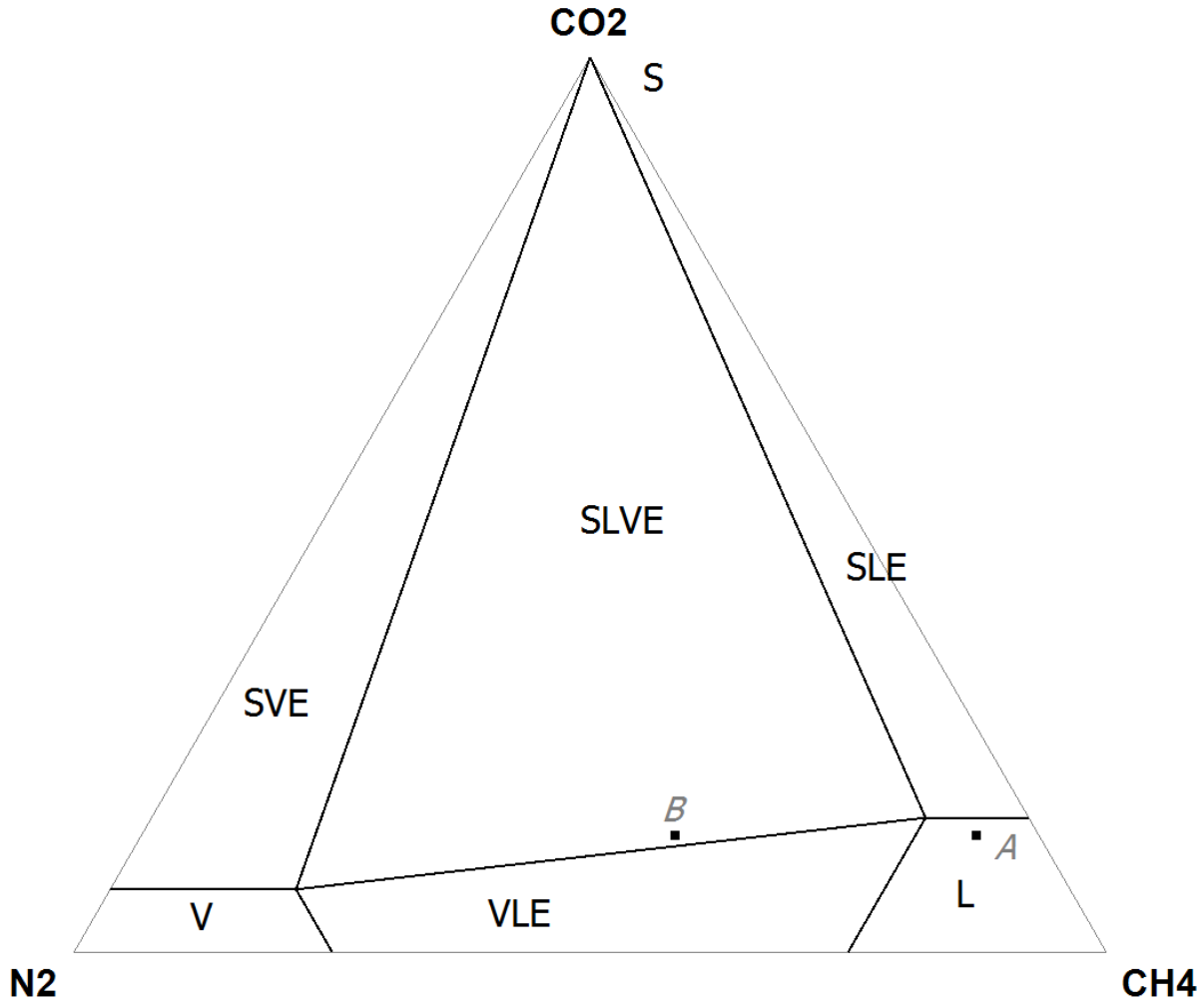

Figure 1. Qualitative phase diagram of the N_2-CH_4-CO_2 system at biomethane liquefaction conditions. S is for solid, L for liquid, and V for vapor phase.

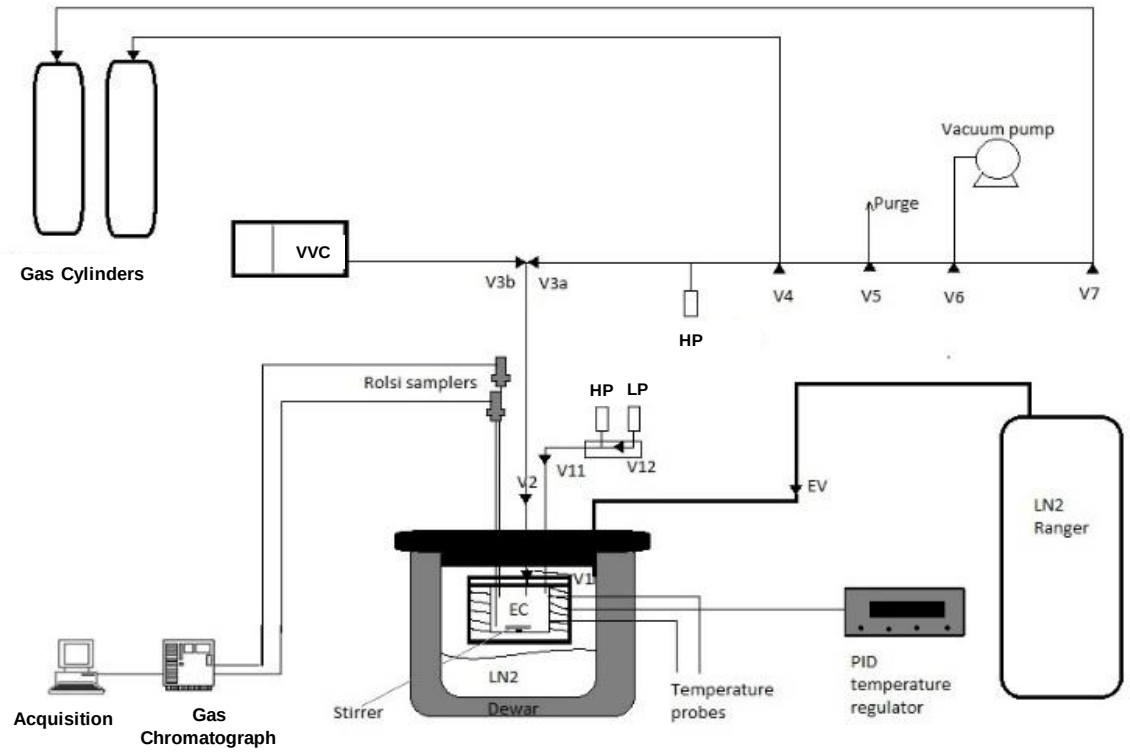

Figure 2. Scheme for the experimental apparatus used in this work. LP: pressure transducer for the low pressure range; EC: equilibrium cell; EV: electrovalve; HP: pressure transducer for the high pressure range; LN2: liquid nitrogen; VVC: variable volume cell; Vi: valves.

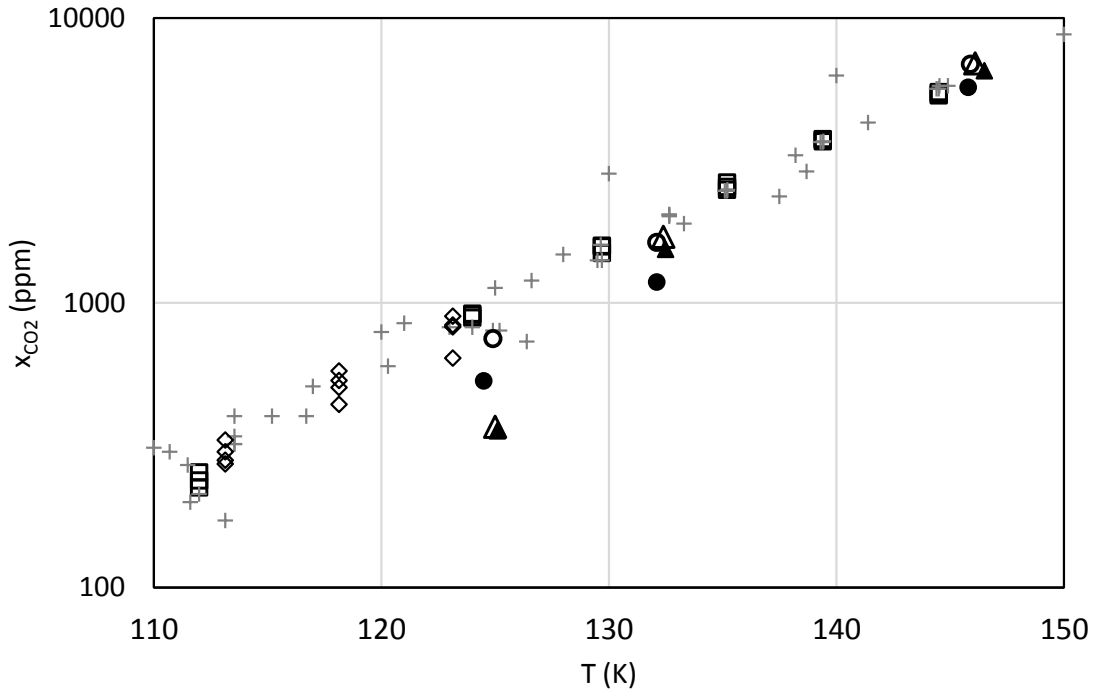

Figure 3. CO_2 Solubility in liquid methane from literature data [4–9] (+), in methane+nitrogen from Shen et al. [1](□), Gao et al. [2] (◊), and from experimental values obtained in this work for the N_2-CH_4-CO_2 system (○ series 1, ● series 2), and the N_2-O_2-CH_4-CO_2 system (Δ series 3, ▲ series 4).

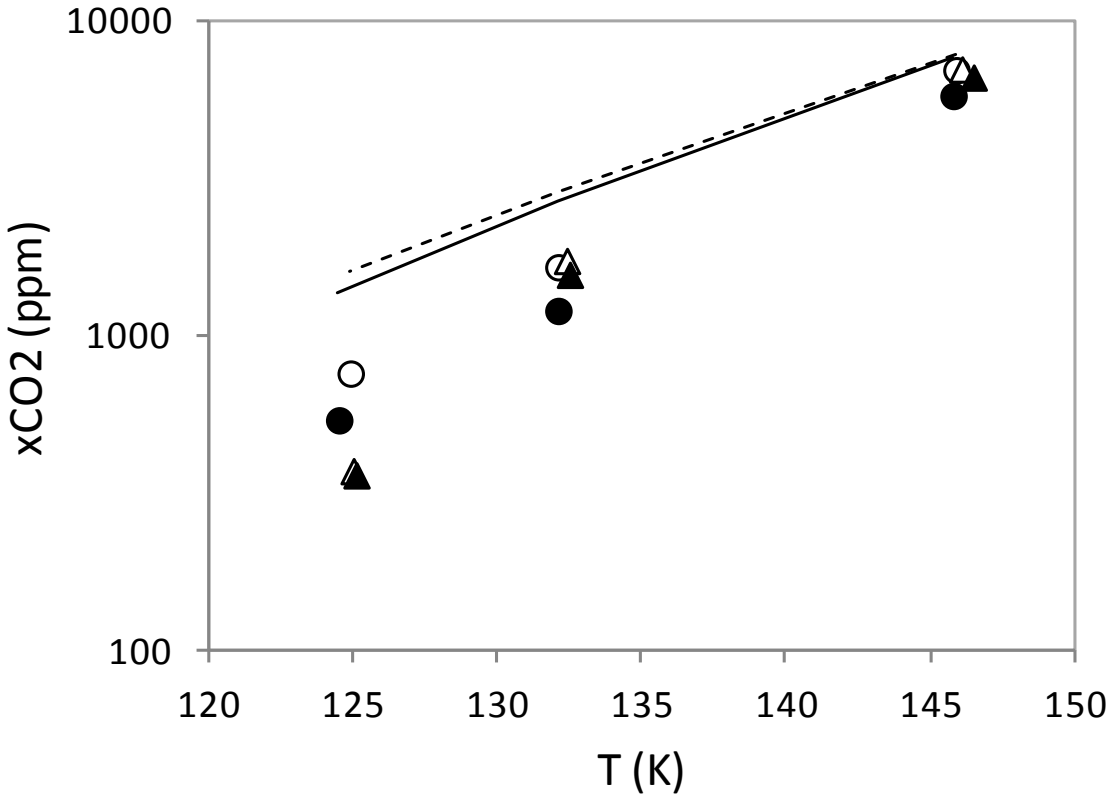

Figure 4. CO_2 solubility in liquid phase (x_{CO2}) at SLVE conditions from experimental values obtained in this work for the N_2-CH_4-CO_2 system (○ series 1, ● series 2), and the N_2-O_2-CH_4-CO_2 system (Δ series 3, ▲ series 4). Results from the model are almost superposed for the ternary and the quaternary system and then they are represented for the ternary system only (--- first series, — second series), for the sake of clarity.

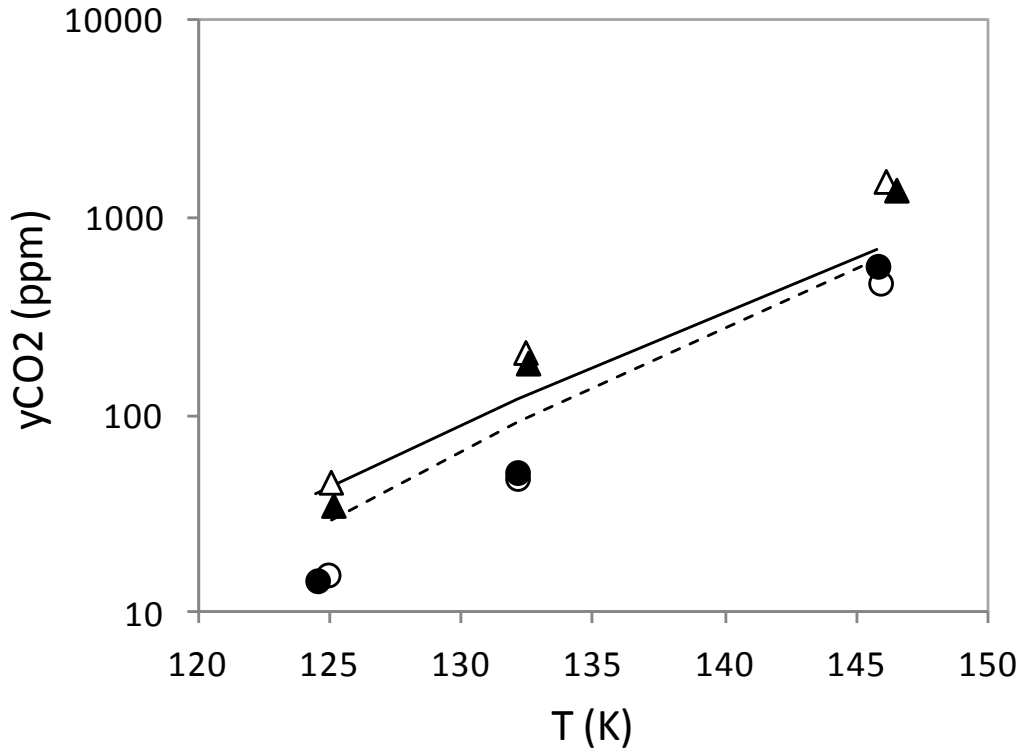

Figure 5. CO_2 solubility in vapor phase (y_{CO2}) at SLVE conditions from experimental values obtained in this work for the N_2-CH_4-CO_2 system (○ series 3, ● series 4), and the N_2-O_2-CH_4-CO_2 system (Δ series 3, ▲ series 4). Results from the model are almost superposed for the ternary and the quaternary system and then they are represented for the ternary system only (--- first series, — second series), for the sake of clarity.

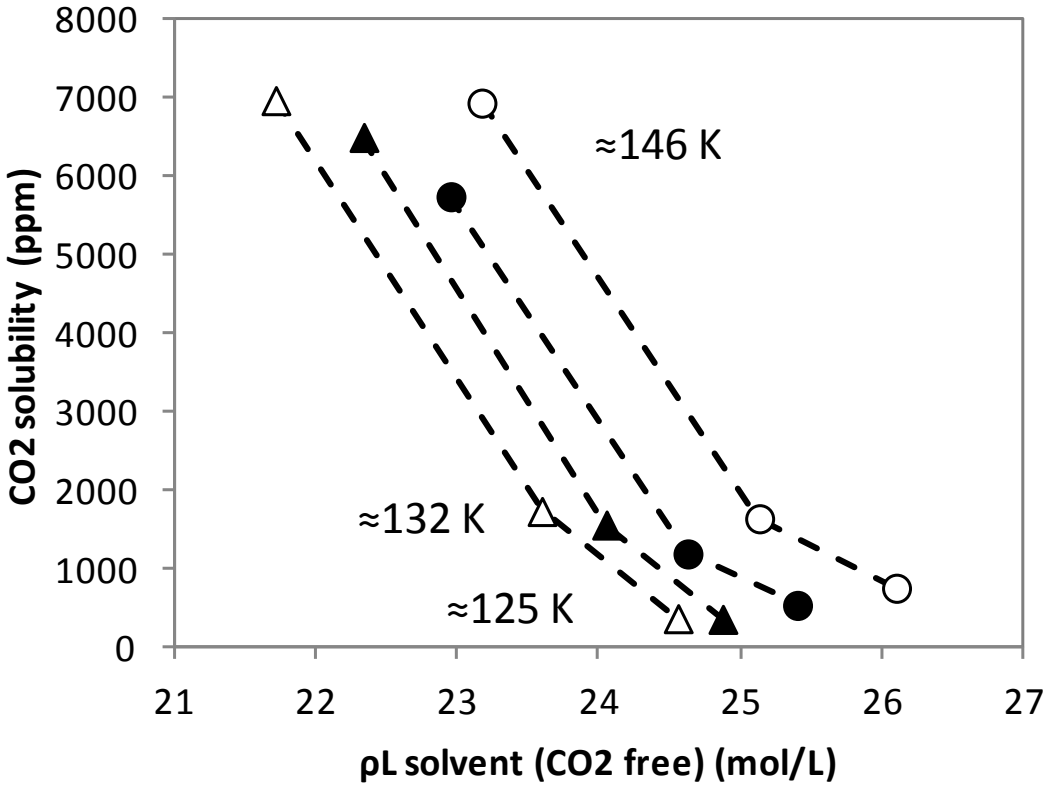

Figure 6. CO_2 solubility in liquid phase with respect to the solvent density (CO_2-free). System N_2-CH_4-CO_2: (○) series 1; (●) series 2. System N_2-O_2-CH_4-CO_2: (Δ) series 3; (▲) series 4. Density is calculated by the model presented in section 3.2. Dotted lines have the only purpose to connect the symbols in the same series in order to highlight the trends.

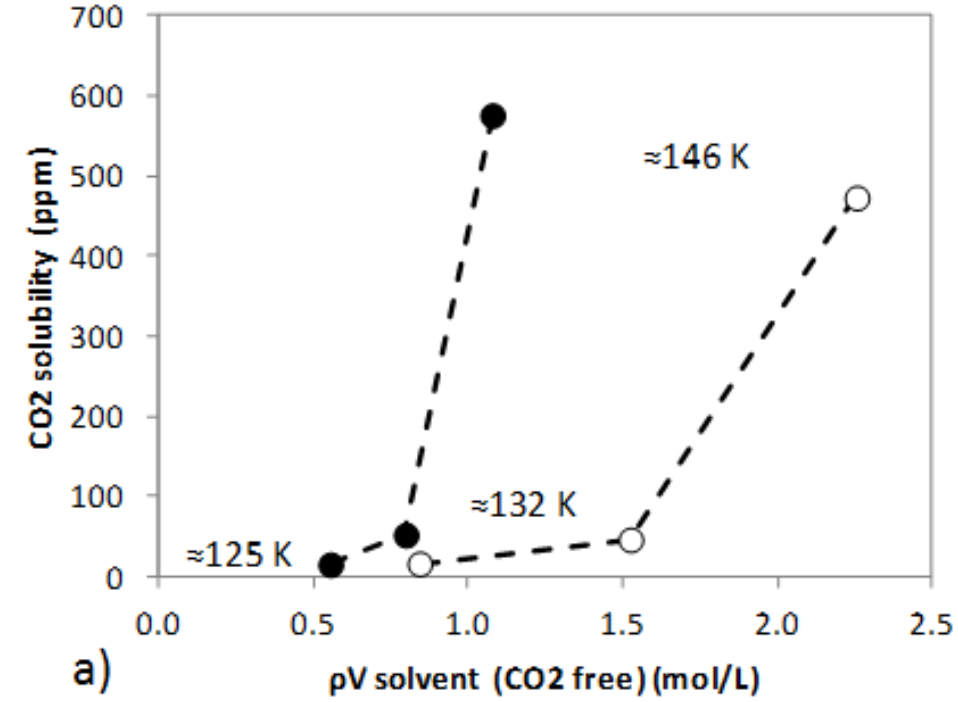
700
600
500
400
300
200
100
0
CO2 solubility (ppm)
≈146 K
≈132 K
≈125 K
0.0
0.5
1.0
1.5
2.0
2.5
ρV solvent (CO2 free) (mol/L)

a)

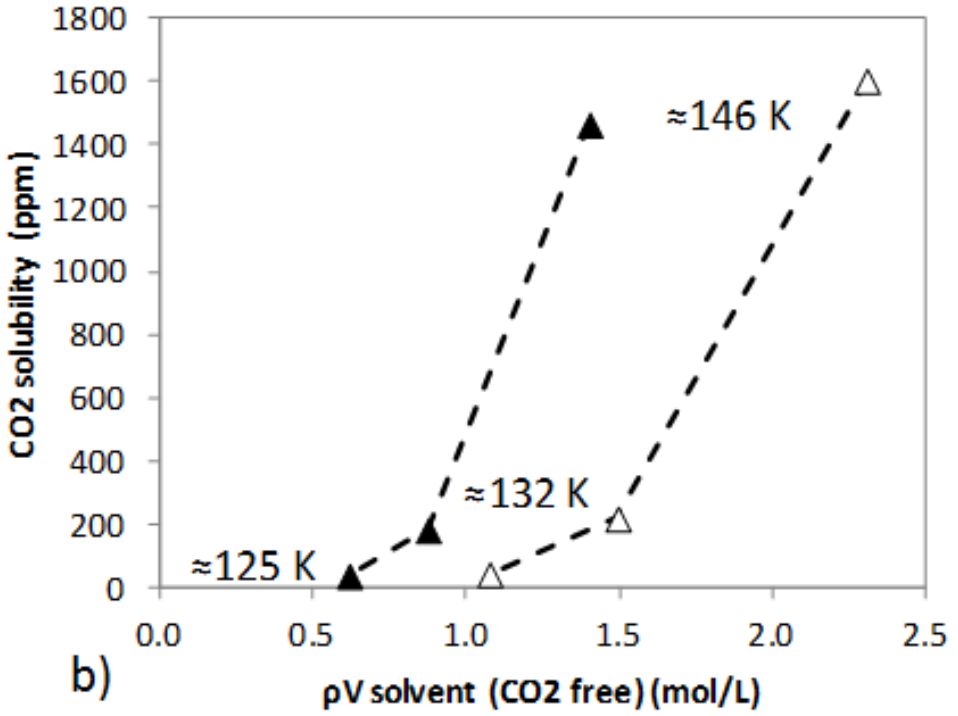
1800
1600
1400
1200
1000
800
600
400
200
0
CO2 solubility (ppm)
≈146 K
≈132 K
≈125 K
0.0
0.5
1.0
1.5
2.0
2.5
ρV solvent (CO2 free) (mol/L)

b)

Figure 7. CO_2 solubility in vapor phase with respect to the solvent density (CO_2-free). a) System N_2-CH_4-CO_2: (○) series 1; (●) series 2. b) System N_2-O_2-CH_4-CO_2: (Δ) series 3; (▲) series 4. Density is calculated by the model presented in section 3.2. Dotted lines have the only purpose to connect the symbols in the same series in order to highlight the trends.